J. Am. Soc. Mass Spectrom. (2016) 27:1376–1382
DOI: 10.1007/s13361-016-1410-4

RESEARCH ARTICLE

Cis→Trans Isomerization of Pro^7 in Oxytocin Regulates Zn^{2+} Binding

Daniel R. Fuller,[1] Matthew S. Glover,[1] Nicholas A. Pierson,[1,2] DoYong Kim,[3] David H. Russell,[3] David E. Clemmer[1]

[1]Department of Chemistry, Indiana University, Bloomington, IN 47405, USA
[2]*Present Address:* Merck Research Laboratories, Rahway, NJ 07065, USA
[3]Department of Chemistry, Texas A&M University, College Station, TX 77842, USA

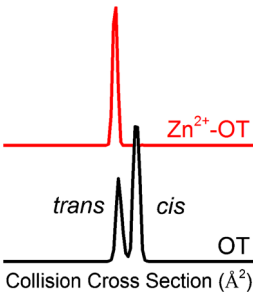

Abstract. Ion mobility/mass spectrometry techniques are employed to investigate the binding of Zn^{2+} to the nine-residue peptide hormone oxytocin (OT, Cys^1-Tyr^2-Ile^3-Gln^4-Asn^5-Cys^6-Pro^7-Leu^8-Gly^9-NH_2, having a disulfide bond between Cys^1 and Cys^6 residues). Zn^{2+} binding to OT is known to increase the affinity of OT for its receptor [Pearlmutter, A. F., Soloff, M. S.: Characterization of the metal ion requirement for oxytocin-receptor interaction in rat mammary gland membranes. J. Biol. Chem. **254**, 3899–3906 (1979)]. In the absence of Zn^{2+}, we find evidence for two primary OT conformations, which arise because the Cys^6–Pro^7 peptide bond exists in both the *trans*- and *cis*-configurations. Upon addition of Zn^{2+}, we determine binding constants in water of K_A = 1.43 ± 0.24 and 0.42 ± 0.12 μM^{-1}, for the *trans*- and *cis*-configured populations, respectively. The Zn^{2+} bound form of OT, having a cross section of Ω = 235 $Å^2$, has Pro^7 in the *trans*-configuration, which agrees with a prior report [Wyttenbach, T., Liu, D., Bowers, M. T.: Interactions of the hormone oxytocin with divalent metal ions. J. Am. Chem. Soc. **130**, 5993–6000 (2008)], in which it was proposed that Zn^{2+} binds to the peptide ring and is further coordinated by interaction of the C-terminal, Pro^7-Leu^8-Gly^9-NH_2, tail. The present work shows that the *cis*-configuration of OT isomerizes to the *trans*-configuration upon binding Zn^{2+}. In this way, the proline residue regulates Zn^{2+} binding to OT and, hence, is important in receptor binding.

Keywords: *Cis-trans* isomerization, Oxytocin, Ion-mobility

Received: 9 March 2016/Revised: 11 April 2016/Accepted: 14 April 2016/Published Online: 6 May 2016

Introduction

Oxytocin (OT) is a nine-residue peptide that facilitates labor and lactation [1], and is associated with psychological issues such as trust, fear, anxiety, aggression, and pair bonding [2, 3]. In the early 1950s, du Vigneaud and his collaborators isolated [4] and synthesized OT [5], as well as determined the sequence as Cys^1-Tyr^2-Ile^3-Gln^4-Asn^5-Cys^6-Pro^7-Leu^8-Gly^9-NH_2, with a disulfide bond between Cys^1 and Cys^6 residues [6], forming a Cys^1-Tyr^2-Ile^3-Gln^4-Asn^5-Cys^6 peptide ring and a Pro^7-Leu^8-Gly^9-NH_2 tail. The structures of the ring and tail are of interest because they are implicated in divalent metal binding, which is known to increase the affinity of OT for its receptor [7]. With this interest, Bowers and coworkers used a combination of ion mobility spectrometry-mass spectrometry (IMS-MS) and theoretical methods to show that when Zn^{2+} binds to OT, it induces a structural change, and they proposed that this was key to the increased receptor affinity for the Zn^{2+}–OT complex [8, 9]. Their calculations suggest two Zn^{2+}–OT structures: one in which Zn^{2+} is octahedrally coordinated with backbone carbonyls associated with six residues (Tyr^2, Ile^3, Gln^4, and Cys^6 of the ring, as well as Leu^8 and Gly^9 of the tail); and another having an additional interaction with the amino terminus [9]. In both of these configurations, the Cys^6–Pro^7 bond adopted a *trans*-orientation, although the *cis*-isomer was not specifically investigated. Electron capture dissociation studies are in agreement with both the ring and tail residues coordinated by Zn [10].

Electronic supplementary material The online version of this article (doi:10.1007/s13361-016-1410-4) contains supplementary material, which is available to authorized users.

Correspondence to: David E. Clemmer; *e-mail:* clemmer@indiana.edu

Although, the prior IMS work did not explicitly consider the presence of *cis*-configured Pro^7 in OT, nuclear magnetic resonance (NMR) studies indicate that a proportion of the Cys^6-Pro^7 bond in OT exists in the *cis*-configuration [11]; several recent studies from our laboratory show that peptides containing a proline residue often exhibit multiple conformations resulting from coexistence of proline in *cis*- and *trans*-configurations [12–16]. Because of this, and the biological importance of understanding the regulation of OT, in this present study we explicitly investigate the role of *cis*- and *trans*-forms of the Pro^7 residue when OT binds to Zn^{2+}. As shown below, we find that, in agreement with the NMR studies [11], the free peptide samples both *cis*- and *trans*-configured proline residues; upon binding the *cis*-isomer of proline must isomerize to the *trans*-isomer, such that the Zn^{2+}-OT complex favors the *trans*-configuration, a final configuration that is consistent with the structure proposed from theory [9]. The *cis*→*trans* isomerization of the Pro^7 residue, which is penultimate to the ring, appears to be important in regulating metal binding, and hence receptor binding.

Experimental

IMS-MS

IMS theory and experimental techniques have been discussed elsewhere [17–22]. In these studies, experiments were performed using a home-built ion mobility spectrometer coupled to a time-of-flight mass spectrometer. Positively charged ions are produced *via* electrospray ionization (ESI) [23] on a Triversa Nanomate (Advion). Ions are then accumulated in a Smith geometry ion funnel [24] and pulsed into a 1.8 m long drift tube. The drift tube is operated with ~3 Torr of He buffer gas at 300 K and a weak electric field (~10 $V \cdot cm^{-1}$). Ions exit the drift tube through a differentially pumped region and are analyzed in the time-of-flight mass spectrometer [25].

Electrospray Ionization for Sampling Solution-Phase Structure

As noted, the present studies utilize ESI to sample biomolecule conformations that exist in solution. A number of studies have shown that populations of peptide and protein conformations observed in the gas phase are related to the populations from solution and under gentle conditions can be monitored by IMS-MS [16, 26–28]. That is, as ions are transferred from solution to the gas phase, information about populations of different conformations from solution is preserved [26, 29, 30]. Silveira et al. implemented cryogenic IMS-MS to provide further insight into how gas phase ions are produced *via* ESI [30]. They and others [26] hypothesize that ions become kinetically trapped by the evaporative cooling process associated with ESI. Therefore, solution-like populations are retained for several milliseconds, which is on the time scale of MS and IMS experiments, making these techniques useful for structural characterization [31, 32].

Assessing Whether IMS Intensities are Due to Solution- or Gas-Phase Populations

While it is often assumed that IMS peak intensities for ions produced by ESI reflect populations found in solution [16, 27, 28], it is important to directly test this, especially for small peptide systems, where ion activation can produce IMS distributions that correspond to "gas-phase" distributions [33]. We test this by gently activating mobility-selected ions and measuring the resulting distributions of structures using an IMS-IMS approach, as described in detail elsewhere [22]. Briefly, IMS-IMS-MS experiments are performed by operating the drift tube as two independent drift regions. Ions are mobility selected in the mid-funnel and are collisionally activated when a high field is applied across a 0.3 cm region. Ions are activated by collisions with the buffer gas and are annealed. Changes in the IMS distributions are then monitored as the new populations are separated in the second drift region.

Determination of Experimental Cross-Section

It is often useful to plot drift time distributions on a cross section scale. Recorded drift times are converted to collisional cross sections (Ω) using [34]:

$$\Omega = \frac{(18\pi)^{1/2}}{16} \frac{ze}{(k_b T)^{1/2}} \left[\frac{1}{m_I} + \frac{1}{m_B}\right]^{1/2} \frac{t_D E}{L} \frac{760}{P} \frac{T}{273.2} \frac{1}{N}, \quad (1)$$

where ze is the charge of the ion, k_b is Boltzmann's constant, m_I is the mass of the ion, m_B is the mass of the buffer gas, t_D is the time required to traverse the drift tube, E is the electric field, L is the drift tube length, T is the temperature, P is the pressure, and N is the neutral number density of the gas at STP.

Peptide Synthesis

Peptides (OT, and the alanine substituted sequence, Cys^1-Tyr^2-Ile^3-Gln^4-Asn^5-Cys^6-Ala^7-Leu^8-Gly^9-NH_2) were synthesized by Fmoc solid-phase synthesis on an Apex 396 peptide synthesizer (AAPPTec, Louisville, KY, USA) as described previously [13]. Fmoc side-chain protected amino acids and Wang-type polystyrene resins were used (Midwest Biotech, Fishers, IN, USA). Deprotections were performed with 20% piperidine in dimethylformamide, and 1,3-Diisopropylcarbodiimide/6-chloro-1-hydroxybenzotriazole was used as the coupling reagent. Peptides were cleaved from the resin with a solution containing trifluoroacetic acid:triisopropylsilane:methanol at a 18:1:1 ratio. Additionally, because the peptides contained cysteine residues, 5% 2,2′-(ethylenedioxy) diethanethiol was added. Peptides were washed, precipitated in diethyl ether, and the products were dried using a vacuum manifold.

Observation of $[OT + Ca]^{2+}$ in the Mass Spectrum

In this study, ESI produces almost exclusively doubly-charged ions of OT (either $[OT+2H]^{2+}$ or $[OT+Zn]^{2+}$). All solutions are sprayed out of water or a mixture of water and methanol. Each sample contains 0.5 μM OT and Zn concentrations ranging from 0 to 6 μM. We note that, although extensive efforts to reduce Ca^{2+} in these experiments have been made, we observe $[OT+Ca]^{2+}$ ions in the mass spectrum. Careful studies of the influence of this contaminant on Zn^{2+} binding have been carried out (see Supplemental Figure 1). The Ca^{2+}-OT abundance does not appear to vary with introduction of Zn^{2+}. Thus it appears to be a spectator in this system, and we do not consider it further.

Determination of Association Constants

The areas under each peak for both $[OT+2H]^{2+}$ and $[OT+Zn]^{2+}$ are integrated after normalization by total ion abundance. The areas of the unbound peaks can then be compared to the areas after addition of Zn^{2+} to determine the fraction bound. Association constants are determined by plotting the fraction of OT bound to Zn^{2+} as a function of the concentration of free Zn^{2+} in solution. The points are fit with a ligand binding, one site saturation model [35] using:

$$f = \frac{B_{max} * [Zn]}{\left({}^{1}/_{K_A} + [Zn] \right)}, \quad (2)$$

where f is the fraction of OT bound to Zn^{2+}, B_{max} is the maximum specific binding, $[Zn]$ is the free Zn^{2+} concentration, and K_A is the association constant.

Results and Discussion

Changes in Conformational Distribution of OT Conformations as a Function of Solution Composition

Figure 1 shows the collision cross section distributions of $[OT+2H]^{2+}$ obtained from different water:methanol solutions. The distribution for $[OT+2H]^{2+}$ shows two peaks, corresponding to populations of structures with collision cross sections of Ω = 236 and 243 Å^2, respectively. In water, the Ω = 236 Å^2 peak comprises ~40% of the distribution. As the amount of methanol in solution is increased, a shift in the distribution occurs, and at the final solution of 95:5 methanol:water, Ω = 236 Å^2 ions are favored, comprising 83% of the distribution. Figure 1 also shows the distribution of conformations at pH 3 in water, which is dominated by Ω = 236 Å^2 ions, comprising ~95% of the distribution. This distribution is interesting because the solution composition is identical to the one reported previously from NMR studies [11, 36], which found two populations corresponding to *cis*- and *trans*-proline configurations at relative abundances of ~10% and ~90%, respectively. The observed changes in the distribution of conformations as a function of solution composition are consistent with

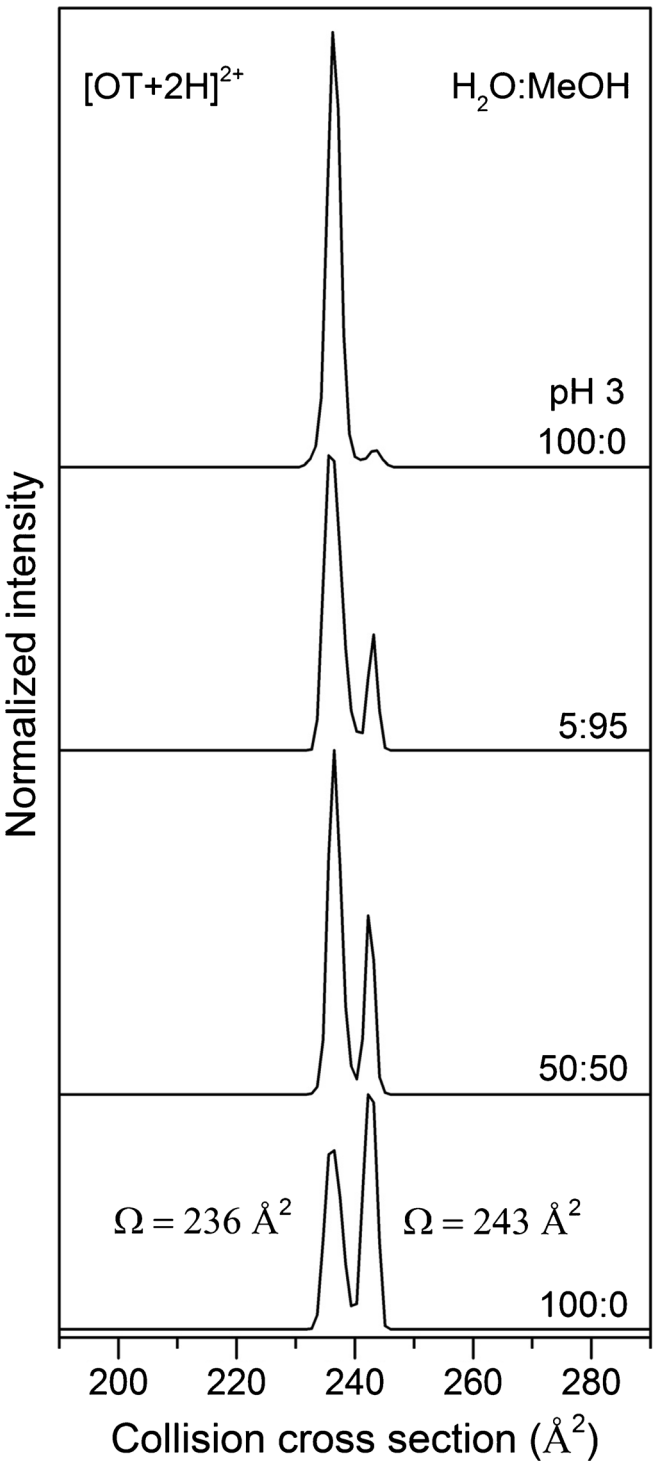

Figure 1. Collision cross section distributions for $[OT+2H]^{2+}$ obtained from different water/methanol solutions. The top trace is the distribution from a pH 3 aqueous solution identical to that used in a NMR study [11]

populations of conformations coming from solution. This agreement suggests that our Ω = 236 and 243 Å^2 peaks correspond to *trans*- and *cis*-isomers, respectively; however, we test this assignment rigorously below.

IMS-IMS-MS of OT

To further understand the relationship of the populations measured in Figure 1 as a function of solution composition, IMS-IMS-MS experiments were conducted. IMS-IMS-MS experiments for mobility selected $[OT+2H]^{2+}$ in Figure 2 show that regardless of which solution is used to produce ions, collisional activation (at our highest energies) results in an identical "gas-phase" distribution. As discussed in detail previously [33], observation of identical populations, regardless of which peak is selected (or which solution is used to produce ions) is evidence for a gas-phase, quasi-equilibrium distribution established in the absence of solvent by collisional activation. This quasi-equilibrium distribution favors the Ω = 236 Å^2 structure, and is clearly different from the distribution produced under gentle ESI conditions, in which the populations are imposed from solution. Figure 2 also shows studies using more gentle activation conditions (60 V) reveal partial conversion of structures, which is consistent with this interpretation. Hereafter, we assume that the distributions recorded from our gentle experimental conditions correspond to solution populations.

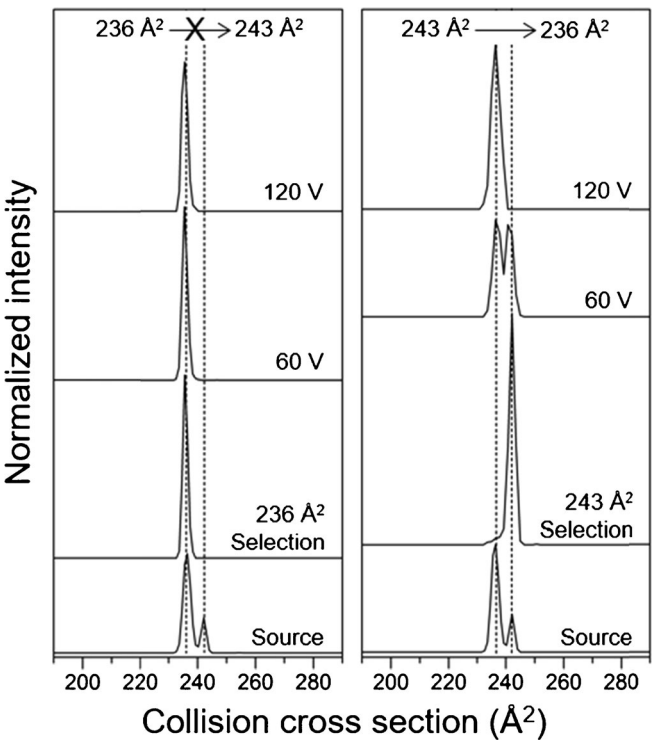

Figure 2. Collision cross section distributions shown for $[OT+2H]^{2+}$ from IMS-IMS-MS experiments. (**a**) Selection and activation of conformation with Ω = 236 Å^2. (**b**) Selection and activation of conformation with Ω = 243 Å^2. The bottom trace for each represents the ESI source distribution from a solution of 50:50 water:methanol with 0.1% FA. Selection and activation experiments were performed by increasing the voltages until dissociation occurs (120 V for OT)

Pro^7→Ala Substitution of OT

As noted above, the abundances of peaks measured for the 100:0 water:methanol solution at pH = 3 are consistent with those reported for the same solution composition by NMR, and suggest assignments of Ω = 236 and 243 Å^2 are *trans*- and *cis*-isomers of Pro^7, respectively. This assignment is rigorously tested by substituting an alanine for the proline to yield Cys^1-Tyr^2-Ile^3-Gln^4-Asn^5-Cys^6-Ala^7-Leu^8-Gly^9-NH_2, in which Cys^6-Ala^7 bond should favor the *trans* configuration [37], as illustrated by the data shown in Figure 3 that displays the collision cross sections for OT (Ala^7) along with OT (Pro^7). Note that the Pro^7→Ala substitution yields a single conformation at 234 Å^2, which makes up ~98% of the distribution. However, since alanine has a smaller intrinsic size parameter, the collision cross section has been corrected to account for the

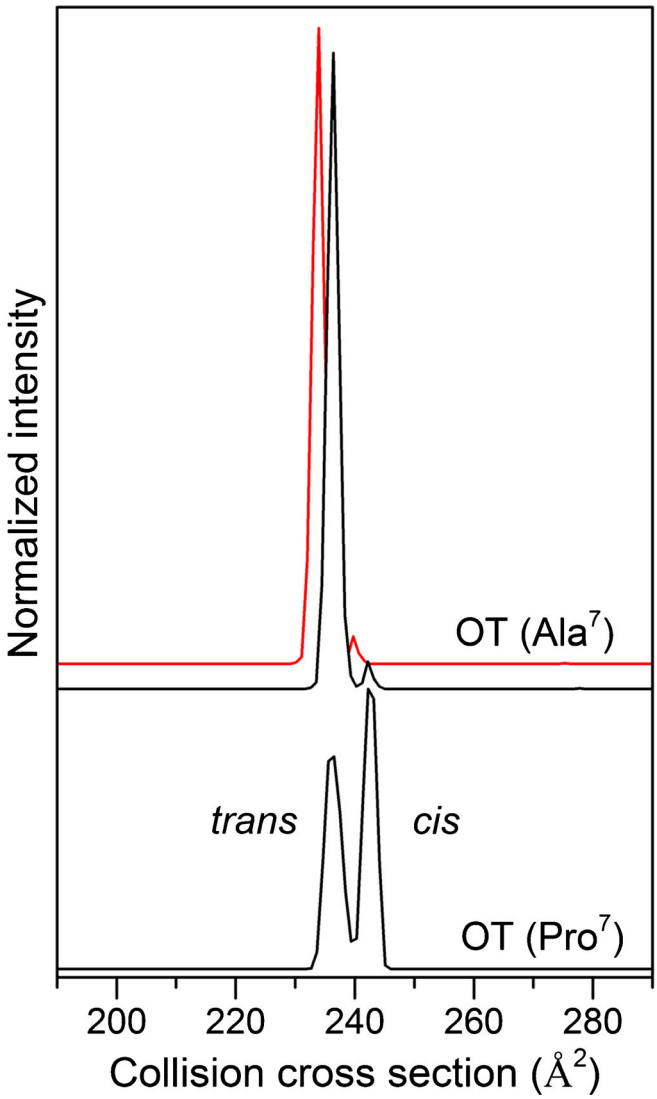

Figure 3. Collision cross section distribution for OT (Pro^7) along with the distribution of OT (Ala^7). For OT (Ala^7), the black trace corresponds to the collision cross section adjusted to correct for the size difference between alanine and proline, and the red trace is the cross section without correction

intrinsic size difference between proline and alanine [38, 39]. The resulting peak has a cross section of 236 $Å^2$. This shows that the Pro^7 residue in the more compact conformation is in the *trans* configuration. The loss in intensity for the $\Omega = 243$ $Å^2$ peak upon alanine substitution indicates that Pro^7 in the elongated conformation is in the *cis*-configuration. Although proline is not penultimate to the N-terminus, it is penultimate to ring, consistent with the importance of penultimate prolines to the conformational heterogeneity of peptides [15, 40].

Determination of Zn^{2+}-OT Association Constants for trans- and cis-OT

Figure 4 shows the collision cross section distributions for $[OT+2H]^{2+}$ and $[OT+Zn]^{2+}$ as a function of Zn^{2+} concentration. Two populations are observed for unbound $[OT+2H]^{2+}$. Solutions with 15 different concentrations of Zn^{2+}, ranging from 0 to 6 μM, have been investigated. The concentration of OT is held constant at 0.5 μM. When no Zn^{2+} is added to solution, the relative abundances of the *trans* ($\Omega = 236$ $Å^2$) and *cis* ($\Omega = 243$ $Å^2$) configurations are ~40% and ~60%, respectively. As more Zn^{2+} is added to solution, the overall abundance of $[OT+2H]^{2+}$ decreases and $[OT+Zn]^{2+}$ is observed in the mass spectrum. Interestingly, as the Zn^{2+} concentration increases, the decrease observed for free OT occurs in a conformation-specific fashion as seen in the mobility distribution. The abundance of the *trans*-configuration decreases relative to the *cis*-configuration, and at the final concentration of Zn^{2+}, the *trans*-configuration comprises ~12% of the total distribution of $[OT+2H]^{2+}$. It should be noted that the collision cross section for the *trans*-configuration in the $[OT+2H]^{2+}$ distribution and the single conformation for $[OT+Zn]^{2+}$ are very similar, suggesting that the Pro^7 bond in OT–Zn complex exists in the *trans*-configuration, which could be the reason that the *trans*-conformation for $[OT+2H]^{2+}$ is favored by Zn^{2+}, in agreement with previous modeling studies on OT–Zn complex [9]. Figure 4 also shows the Zn bound form of OT is comprised of only one peak with $\Omega = 235$ $Å^2$. These data suggest that zinc binds to the multiple OT conformations, and adds rigidity to the molecule, which is evident by one prominent peak in the collision cross section distribution. This further elucidates why zinc increases the affinity of OT to its receptor; it not only imposes a structural change to OT but it also gathers the multiple conformations of a dynamic peptide and adopts just one upon binding.

Differences in binding affinities for Zn^{2+} to the two prominent conformations for $[OT+2H]^{2+}$ can be calculated because of the conformational-specific binding. Many studies have been performed to determine binding constants for various protein–ligand complexes with ESI-MS [41–46]. In this study, we use IMS-MS data to calculate K_As for Zn^{2+} bound to OT. Figure 5 shows the results from the fit of the titration data for both the *cis*- and *trans*-configurations of Pro^7 in OT. To obtain this plot, we integrate the area under the peaks corresponding to each conformation in the mobility distribution for $[OT+2H]^{2+}$ and $[OT+Zn]^{2+}$. From this, we can relate the drop in abundance

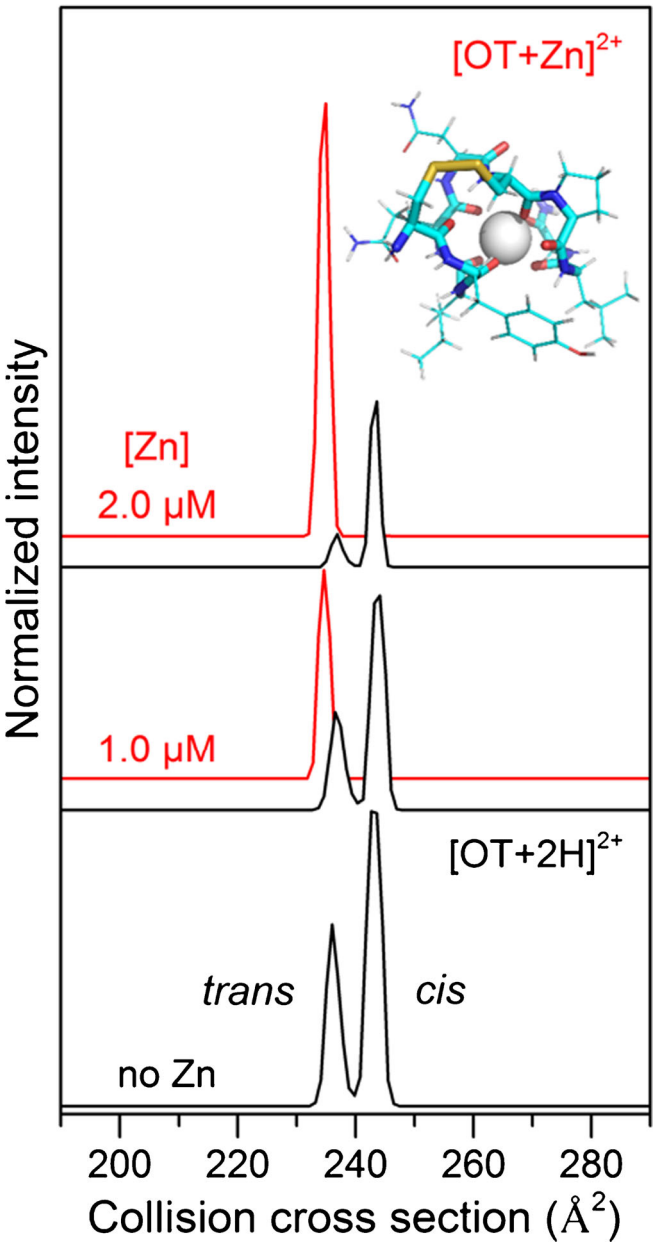

Figure 4. Collision cross section distributions for $[OT+2H]^{2+}$ and $[OT+Zn]^{2+}$. $[OT+2H]^{2+}$ distributions are displayed as the black trace and $[OT+Zn]^{2+}$ distributions as the red trace. The concentration of Zn (μM) is displayed on the left side of each trace. Distributions are normalized by total abundance of $[OT+2H]^{2+}$ and $[OT+Zn]^{2+}$. OT-Zn complex structure is adapted from ref. [9]

for each conformation as the concentration of Zn^{2+} increases, to the individual conformers' contribution to the OT–Zn complex. From the data in Figure 5, we determine binding affinities for the *trans*- and *cis*-configurations with Zn^{2+} to be 1.43 ± 0.24 μM^{-1} and 0.42 ± 0.12 μM^{-1}, respectively. Thus, the affinity of OT for Zn^{2+}, when Pro^7 exists as the *trans*-isomer, is more than three times greater than when Pro^7 exists as the *cis*-isomer. This difference in affinity ultimately requires that the *cis*-configuration isomerizes to the *trans*-isomer to stabilize

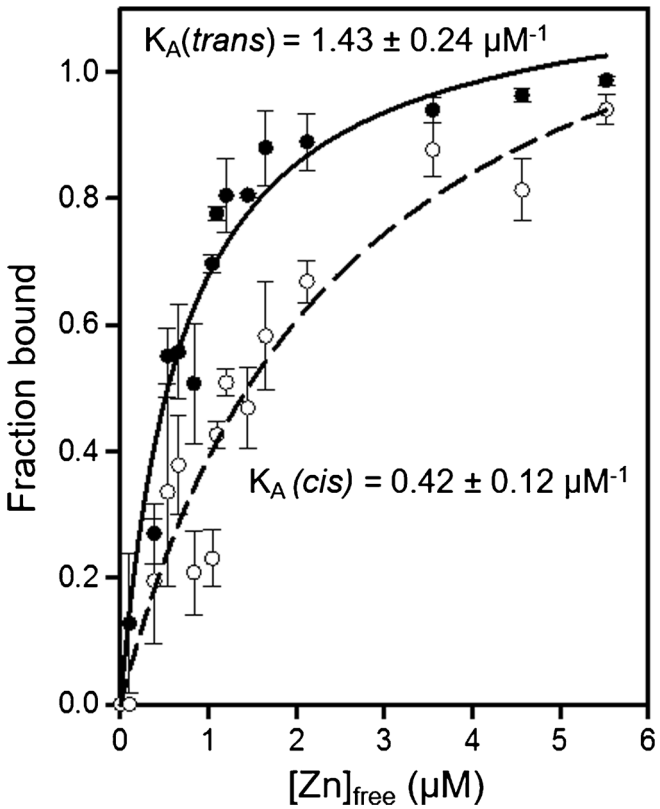

Figure 5. K_As for the individual conformations of OT with Zn. The fraction bound of OT is plotted as a function of free Zn^{2+} concentration (μM). The solid curve is the fit for the *trans* configuration data and the dashed line is the fit for the *cis* configuration data

the Zn^{2+}-bound structure. The final *trans*-Pro Zn^{2+}-OT structure is consistent with the theoretical structures proposed by Bowers and coworkers [9].

There are two mechanisms to consider when discussing ligand binding: conformational selection [47, 48] and induced fit [49–51]. In conformational selection, a biomolecule may sample many structures along its energy landscape, and binding occurs through selection by the ligand to a preferred unbound conformation while maintaining similar structure. In the induced fit mechanism, the ligand binds to the unbound conformation and induces a specific structural change. From our scenario it is not hard to imagine both mechanisms involved in the binding process. Because the unbound *trans*-isomer has a similar cross section to that of the bound complex, the mechanism could be classified as conformational selection. However, we also observe the depletion of the *cis*-isomer when Zn is added to solution. In one case, a *cis*→*trans* isomerization could occur prior to Zn^{2+} binding, allowing Zn^{2+} to bind to the preferred structure, maintaining the conformational selection mechanism. However, there is also a scenario where Zn^{2+} could bind to the *cis*-isomer, inducing a *cis*→*trans* isomerization, which would then be considered under the induced fit mechanism. It is reasonable to assume that a combination of both exist in this system; however, our experimental approach cannot distinguish between the two possible mechanisms.

Cis→Trans Isomerization of Proline Regulates Zn^{2+} Binding

Ultimately, the studies presented above (and prior NMR studies [11]) show that the proline residue in OT gives rise to a conformational heterogeneity that varies substantially in different solution environments. Thus, in some environments where the *cis*-isomer is favored, it will be the case that *cis*→*trans* isomerization of proline regulates Zn^{2+} binding, and thus directly affects receptor affinity. This new finding suggests that mutations (e.g., OT sequences in which the proline residue is replaced with a *trans*-favoring residue such as alanine) may influence receptor binding and, hence, physiological efficacy of OT in environments where the *trans* form is not favored for proline. Studies that examine related sequences would be interesting.

Conclusions

IMS-MS studies find that OT adopts multiple conformations in solution due to *cis-trans* isomerization of the Cys^6–Pro^7 bond. Upon binding Zn^{2+} to OT, the *cis*-isomer converts to the *trans*-isomer; this differences leads to unique binding affinities for the *trans*- and *cis*-configurations with Zn^{2+} of $K_A = 1.43 \pm 0.24\ \mu M^{-1}$ and $0.42 \pm 0.12\ \mu M^{-1}$, respectively. While previous studies have qualitatively demonstrated conformation specific binding of a ligand to a biomolecule [52, 53], we used IMS-MS techniques to resolve and quantify differences in binding affinities that are associated with different structures. The structural transition that occurs in this system suggests that the proline residue regulates Zn^{2+} binding to OT in environments where the *cis*-isomer of proline is favored in the Zn^{2+}-free OT form. This finding suggests that a more efficacious form of OT (at least in terms of metal- and presumably receptor-binding interactions in *cis*-isomer favoring environments) might be created by removing the ability of the peptide to form the *cis*-isomer; e.g., one can imagine introducing a mutation at the 7th residue in which the proline residue is replaced by amino acids, which favor *trans*-isomer configurations. We note that while the OT sequence is highly conserved across many types of organisms [1], other biologically active peptides (e.g., vasopressin and vasotocin) incorporate similar ring structures with a proline residue that is penultimate to the ring that may show similar behavior. We are currently investigating these systems.

Acknowledgments

The authors acknowledge David Smiley and the DiMarchi research group at Indiana University for assistance with the peptide synthesis. This work is supported by a grant from the NIH (R01 GM103725).

References

1. Gimpl, G., Fahrenholz, F.: The oxytocin receptor system: structure, function, and regulation. Physiol. Rev. **81**, 629–683 (2001)
2. Winslow, J.T., Hastings, N., Carter, S., Harbaugh, C.R., Insel, T.R.: A role for central vasopressin in pair bonding in monogamous prairie voles. Nature **365**, 7 (1993)

3. Barberis, C., Mouillac, B., Durroux, T.: Structural bases of vasopressin/oxytocin receptor function. J. Endocrinol. **156**, 223–229 (1998)
4. Livermore, A.H., du Vigneaud, V.: Preparation of high potency oxytocic material by the use of counter-current distribution. J. Biol. Chem. **180**, 365–373 (1949)
5. du Vigneaud, V., Ressler, C., Swan, J.M., Roberts, C.W., Katsoyannis, P.G.: The synthesis of oxytocin. J. Am. Chem. Soc. **76**, 3115–3121 (1954)
6. du Vigneaud, V., Ressler, C., Trippett, S.: The sequence of amino acids in oxytocin, with a proposal for the structure of oxytocin. J. Biol. Chem. **205**, 949–957 (1953)
7. Pearlmutter, A.F., Soloff, M.S.: Characterization of the metal ion requirement for oxytocin–receptor interaction in rat mammary gland membranes. J. Biol. Chem. **254**, 3899–3906 (1979)
8. Liu, D., Seuthe, A.B., Ehrler, O.T., Zhang, X., Wyttenbach, T., Hsu, J.F., Bowers, M.T.: Oxytocin-receptor binding: why divalent metals are essential. J. Am. Chem. Soc. **127**, 2024–2025 (2005)
9. Wyttenbach, T., Liu, D., Bowers, M.T.: Interactions of the hormone oxytocin with divalent metal ions. J. Am. Chem. Soc. **130**, 5993–6000 (2008)
10. Kleinnijenhuis, A.J., Mihalca, R., Heeren, R.M., Heck, A.J.: Atypical behavior in the electron capture induced dissociation of biologically relevant transition metal ion complexes of the peptide hormone oxytocin. Int. J. Mass Spectrom. **253**, 217–224 (2006)
11. Larive, C.K., Guerra, L., Rabenstein, D.L.: *Cis/trans* conformational equilibrium across the cysteine 6-proline peptide bond of oxytocin, arginine vasopressin, and lysine vasopressin. J. Am. Chem. Soc. **114**, 7331–7337 (1992)
12. Counterman, A.E., Clemmer, D.E.: *Cis-trans* signatures of proline-containing tryptic peptides in the gas phase. Anal. Chem. **74**, 1946–1951 (2002)
13. Pierson, N.A., Chen, L., Russell, D.H., Clemmer, D.E.: *Cis-trans* isomerizations of proline residues are key to bradykinin conformations. J. Am. Chem. Soc. **135**, 3186–3192 (2013)
14. Shi, L., Holliday, A.E., Shi, H., Zhu, F., Ewing, M.A., Russell, D.H., Clemmer, D.E.: Characterizing intermediates along the transition from polyproline I to polyproline II using ion mobility spectrometry-mass spectrometry. J. Am. Chem. Soc. **136**, 12702–12711 (2014)
15. Glover, M.S., Shi, L., Fuller, D.R., Arnold, R.J., Radivojac, P., Clemmer, D.E.: On the split personality of penultimate proline. J. Am. Soc. Mass Spectrom. **26**, 444–452 (2015)
16. Glover, M.S., Bellinger, E.P., Radivojac, P., Clemmer, D.E.: Penultimate proline in neuropeptides. Anal. Chem. **87**, 8466–8472 (2015)
17. Clemmer, D.E., Jarrold, M.F.: Ion mobility measurements and their applications to clusters and biomolecules. J. Mass Spectrom. **32**, 577–592 (1997)
18. St. Louis, R.H., Hill Jr., H.H., Eiceman, G.A.: Ion mobility spectrometry in analytical chemistry. Crit. Rev. Anal. Chem. **21**, 321–355 (1990)
19. Wyttenbach, T., von Helden, G., Batka, J.J., Carlat, D., Bowers, M.T.: Effect of the long-range potential on ion mobility measurements. J. Am. Soc. Mass Spectrom. **8**, 275–282 (1997)
20. Wyttenbach, T., Kemper, P.R., Bowers, M.T.: Design of a new electrospray ion mobility mass spectrometer. Int. J. Mass Spectrom. **212**, 13–23 (2001)
21. Koeniger, S.L., Merenbloom, S.I., Valentine, S.J., Jarrold, M.F., Udseth, H.R., Smith, R.D., Clemmer, D.E.: An IMS-IMS analogue of MS-MS. Anal. Chem. **78**, 4161–4174 (2006)
22. Merenbloom, S.I., Koeniger, S.L., Valentine, S.J., Plasencia, M.D., Clemmer, D.E.: IMS-IMS and IMS-IMS-IMS/MS for separating peptide and protein fragment ions. Anal. Chem. **78**, 2802–2809 (2006)
23. Fenn, J.B., Mann, M., Meng, C.K., Wong, S.F., Whitehouse, C.M.: Electrospray ionization for mass spectrometry of large biomolecules. Science **246**, 64–71 (1989)
24. Tang, K., Shvartsburg, A.A., Lee, H.-N., Prior, D.C., Buschbach, M.A., Li, F., Tolmachev, A.V., Anderson, G.A., Smith, R.D.: High-sensitivity ion mobility spectrometry/mass spectrometry using electrodynamic ion funnel interfaces. Anal. Chem. **77**, 3330–3339 (2005)
25. Hoaglund, C.S., Valentine, S.J., Sporleder, C.R., Reilly, J.P., Clemmer, D.E.: Three-dimensional ion mobility/TOFMS analysis of electrosprayed biomolecules. Anal. Chem. **70**, 2236–2242 (1998)
26. Lee, S.-W., Freivogel, P., Schindler, T., Beauchamp, J.: Freeze-dried biomolecules: FT-ICR studies of the specific solvation of functional groups and clathrate formation observed by the slow evaporation of water from hydrated peptides and model compounds in the gas phase. J. Am. Chem. Soc. **120**, 11758–11765 (1998)
27. Pierson, N.A., Chen, L., Valentine, S.J., Russell, D.H., Clemmer, D.E.: Number of solution states of bradykinin from ion mobility and mass spectrometry measurements. J. Am. Chem. Soc. **133**, 13810–13813 (2011)
28. Wyttenbach, T., Bowers, M.T.: Structural stability from solution to the gas phase: native solution structure of ubiquitin survives analysis in a solvent-free ion mobility-mass spectrometry environment. J. Phys. Chem. B **115**, 12266–12275 (2011)
29. Rodriguez-Cruz, S.E., Klassen, J.S., Williams, E.R.: Hydration of gas-phase gramicidin S (M+2H) 2+ ions formed by electrospray: the transition from solution to gas-phase structure. J. Am. Soc. Mass Spectrom. **8**, 565–568 (1997)
30. Silveira, J.A., Fort, K.L., Kim, D., Servage, K.A., Pierson, N.A., Clemmer, D.E., Russell, D.H.: From solution to the gas phase: stepwise dehydration and kinetic trapping of Substance P reveals the origin of peptide conformations. J. Am. Chem. Soc. **135**, 19147–19153 (2013)
31. Bohrer, B.C., Merenbloom, S.I., Koeniger, S.L., Hilderbrand, A.E., Clemmer, D.E.: Biomolecule analysis by ion mobility spectrometry. Annu. Rev. Anal. Chem. **1**, 293 (2008)
32. Wyttenbach, T., Pierson, N.A., Clemmer, D.E., Bowers, M.T.: Ion mobility analysis of molecular dynamics. Annu. Rev. Phys. Chem. **65**, 175–196 (2014)
33. Pierson, N.A., Valentine, S.J., Clemmer, D.E.: Evidence for a quasi-equilibrium distribution of states for bradykinin $[M+3H]^{3+}$ ions in the gas phase. J. Phys. Chem. B **114**, 7777–7783 (2010)
34. Mason, E.A., McDaniel, E.W.: Transport Properties of Ions in Gases, pp. 1–29. Wiley, New York (1988)
35. Sigmaplot, version 13.0. Systat Software Inc., San Jose (2014)
36. Larive, C.K., Rabenstein, D.L.: Dynamics of *cis/trans* isomerization of the cysteine 6-proline peptide bonds of oxytocin and arginine-vasopressin in aqueous and methanol solutions. J. Am. Chem. Soc. **115**, 2833–2836 (1993)
37. Stewart, D.E., Sarkar, A., Wampler, J.E.: Occurrence and role of cis peptide bonds in protein structures. J. Mol. Biol. **214**, 253–260 (1990)
38. Valentine, S.J., Counterman, A.E., Hoaglund-Hyzer, C.S., Clemmer, D.E.: Intrinsic amino acid size parameters from a series of 113 lysine-terminated tryptic digest peptide ions. J. Phys. Chem. B **103**, 1203–1207 (1999)
39. Srebalus Barnes, C.A., Clemmer, D.E.: Assessing intrinsic side chain interactions between i and i + 4 residues in solvent-free peptides: a combinatorial gas-phase approach. J. Phys. Chem. B **107**, 10566–10579 (2003)
40. Voet, D., Voet, J.G.: Biochemistry. Wiley, New York (1995)
41. Loo, J.A., Hu, P., McConnell, P., Mueller, W.T., Sawyer, T.K., Thanabal, V.: A study of Src SH2 domain protein-phosphopeptide binding interactions by electrospray ionization mass spectrometry. J. Am. Soc. Mass Spectrom. **8**, 234–243 (1997)
42. Kempen, E.C., Brodbelt, J.S.: A method for the determination of binding constants by electrospray ionization mass spectrometry. Anal. Chem. **72**, 5411–5416 (2000)
43. Gao, H., Yu, Y., Leary, J.A.: Mechanism and kinetics of metalloenzyme phosphomannose isomerase: measurement of dissociation constants and effect of zinc binding using ESI-FTICR mass spectrometry. Anal. Chem. **77**, 5596–5603 (2005)
44. Wilcox, J.M., Rempel, D.L., Gross, M.L.: Method of measuring oligonucleotide-metal affinities: interactions of the thrombin binding aptamer with K+ and Sr2+. Anal. Chem. **80**, 2365–2371 (2008)
45. Di Marco, V.B., Bombi, G.G., Zambon, S., Traldi, P.: Metal–ligand solution equilibria studied by electrospray ionization mass spectrometry: effect of instrumental parameters. J. Mass Spectrom. **44**, 120–127 (2009)
46. Cubrilovic, D., Biela, A., Sielaff, F., Steinmetzer, T., Klebe, G., Zenobi, R.: Quantifying protein-ligand binding constants using electrospray ionization mass spectrometry: a systematic binding affinity study of a series of hydrophobically modified trypsin inhibitors. J. Am. Soc. Mass Spectrom. **23**, 1768–1777 (2012)
47. Monod, J., Wyman, J., Changeux, J.P.: On the nature of allosteric transitions: a plausible model. J. Mol. Biol. **12**, 88–118 (1965)
48. Vogt, A.D., Di Cera, E.: Conformational selection is a dominant mechanism of ligand binding. Biochemistry **52**, 5723–5729 (2013)
49. Koshland, D.E.: Application of a theory of enzyme specificity to protein synthesis. Proc. Natl. Acad. Sci. U. S. A. **44**, 98–104 (1958)
50. Goh, C.S., Milburn, D., Gerstein, M.: Conformational changes associated with protein–protein interactions. Curr. Opin. Struct. Biol. **14**, 104–109 (2004)
51. Kim, E., Lee, S., Jeon, A., Choi, J.M., Lee, H.S., Hohng, S., Kim, H.S.: A single-molecule dissection of ligand binding to a protein with intrinsic dynamics. Nat. Chem. Biol. **9**, 313–318 (2013)
52. Ruotolo, B.T., Tate, C.C., Russell, D.H.: Ion mobility-mass spectrometry applied to cyclic peptide analysis: conformational preferences of gramicidin S and linear analogs in the gas phase. J. Am. Soc. Mass Spectrom. **15**, 870–878 (2004)
53. Illes-Toth, E., Dalton, C.F., Smith, D.P.: Binding of dopamine to alpha-synuclein is mediated by specific conformational states. J. Am. Soc. Mass Spectrom. **24**, 1346–1354 (2013)